Synthesis of Ethylene/1-Octene Copolymers with Controlled Block Structures by Semibatch Living Copolymerization

Weifeng Liu, Song Guo, Hong Fan, Wenjun Wang, and Bo-Geng Li
Dept. of Chemical and Biological Engineering, State Key Laboratory of Chemical Engineering, Zhejiang University, Hangzhou 310027, P.R. China

Shiping Zhu
Dept. of Chemical Engineering, McMaster University, Hamilton, ON, Canada, L8S 4L7

DOI 10.1002/aic.14204
Published online August 9, 2013 in Wiley Online Library (wileyonlinelibrary.com)

A kinetic model was developed for the living copolymerization of ethylene/1-octene using the fluorinated FI-Ti catalyst system, bis[N-(3-methylsalicylidene)-2,3,4,5,6-pentafluoroanilinato] $TiCl_2$/dried methylaluminoxane is presented. The model was first validated by batch polymerization experiments. Kinetic parameters were estimated from the model correlations with online ethylene consumption rates and end-of-batch copolymer molecular weight. The model was then used to calculate the microstructural properties of ethylene/1-octene copolymers with controlled composition profiles (uniform, diblock, and step triblock), which were synthesized using sequential comonomer feeding policies in semibatch copolymerization. The synthesized block copolymers had the exact composition distributions and molecular weights as the model simulated. It was demonstrated that the polymer chain microstructure in the living copolymerization of olefins could be precisely regulated by using semibatch comonomer feeding policies. © 2013 American Institute of Chemical Engineers *AIChE J*, 59: 4686–4695, 2013

Keywords: polymerization, reaction kinetics, modeling, living copolymerization, olefin block copolymers

Introduction

Molecular weight and chain microstructure are two factors that, to a large extent, determine materials' properties and final applications of polymers. For polyolefins produced with coordination catalysts, it is well-known that chain microstructure is determined by catalyst type. Over decades, numerous efforts have been spent in developing new catalysts for targeted chain microstructure.[1] It is probably less recognized that reaction engineering also plays an important role in determining chain microstructure.[2] Different processes yield different products in polyolefin production, even with the same catalyst. Kinetic study is an essential part in polymer reaction engineering. Combination of modeling and experimentation represents a most powerful approach in the kinetic study of polymerization.[3] A good kinetic model can help to establish the relationships between reaction conditions and chain microstructural properties of resulting polymers.[4,5] Modeling also facilitates understanding and elucidation of the polymerization mechanisms.[6] Furthermore, in the olefin copolymerization, kinetic models can be used to design and control polyolefin chain microstructure.[7]

In controlled/living radical copolymerization, kinetic models have been used in designing copolymer molecular weight and composition, targeting for novel material properties.[8] For examples, a series of styrene/butyl acrylate copolymers having well-controlled composition distribution along chain backbones were prepared via a reversible addition-fragmentation chain transfer polymerization (RAFT), on the basis of a semibatch kinetic model design.[9] The copolymer samples having different composition profiles from one chain end to another gave very different thermal properties, even with a same average composition. Through semibatch modeling, Luo et al.[10] also synthesized via RAFT polymerization a series of precisely designed triblock copolymers of styrene, *n*-butylacrylate, and styrene, which exhibited thermoplastic elastomeric properties. It was demonstrated that the ultimate tensile strength of these triblock copolymers was solely determined by their composition. The microstructural properties of copolymers could also be controlled by atom transfer radical polymerization through a model-based semibatch design.[11] Luo and coworkers[12] synthesized methyl methacrylate/tert-butyl methacrylate copolymers having linear and hyperbolic gradient composition profiles. These examples have shown that kinetic modeling and semibatch control provide a powerful tool in the precision synthesis of tailor-made copolymer products in the controlled/living radical polymerization.

Over the decade, remarkable progresses have also been achieved in living olefin polymerization.[13] Significant advances have been obtained in the control of polyolefin chain microstructure via living polymerization mechanisms. Polyolefin samples having complex chain architectures have been synthesized, such as star polyethylenes,[14] hyperbranched polyethylenes,[15] olefin block copolymers,[16,17] and so forth, which could not be prepared from the traditional coordination polymerization. Since late 1990's, living coordination catalyst systems have attracted much attention in the research community.[13] As

Correspondence concerning this article should be addressed to B.-G. Li at bgli@zju.edu.cn or to S. Zhu at zhuship@mcmaster.ca.

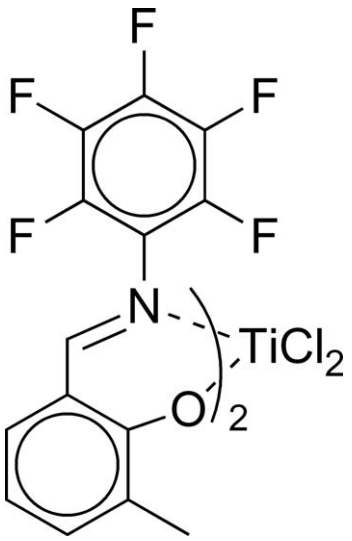

Scheme 1. The structure of the fluorinated FI-Ti catalyst used in this work.

the β-H chain transfer reactions are limited, the fluorinated FI catalyst is among the most efficient living catalyst systems.[18] Using this catalyst, ethylene/propylene and ethylene/1-hexene block copolymers were prepared.[16,17,19] These block copolymers exhibited superior extensibility and toughness compared to their random counterparts.[20] However, kinetic modeling, an important reaction engineering tool, has not been extensively applied in living olefin polymerization systems for precise control over polyolefin chain microstructure.

Recently, we investigated copolymerization of ethylene with 1-octene using a fluorinated FI-Ti catalyst system. The living copolymerization behavior of this catalyst system has been clearly demonstrated in our previous work.[21] The living feature was retained at an extremely high comonomer level. In this study, we used a modeling approach coupled with experimental work targeting at precise control over chain microstructure of polyolefins through the living coordination polymerization. It is believed that there are still a lot to explore with polyolefins if microstructure of individual chains can be précised designed and controlled. Digital synthesis and precision production would result in novel polyolefin products with desired tailor-made properties.

A kinetic model is developed for the living ethylene/1-octene copolymerization system. The kinetic parameters are estimated from model correlation with batch experimental results. The model is then used to simulate the chain microstructural profiles of the living ethylene/1-octene block copolymers, which are validated by experimental results.

Experimental Section

Materials and preparation

The experimental procedure has mostly been described in our previous article.[21] We repeat it here for reader's convenience. All the air- and/or moisture-sensitive materials were manipulated through standard Schlenk techniques or in a high-purity nitrogen-filled glovebox. Toluene (HPLC/Spectro grade, Tedia Company) was refluxed over sodium/potassium for more than 24 h before use. It was under the protection of nitrogen with benzophenone as an indicator. 1-Octene (99+%, Acros Organics) was also distilled over sodium under nitrogen for 3 h and was then sealed with molecular sieves and stored in glove-box. Polymerization-grade ethylene (Sinopec Yangzi Petrochemical Company Ltd) was purified by sequentially passing through columns filled with CuO, 5A molecular sieves and ascarite. The purification columns and glovebox were reactivated every 2 months. Methylaluminoxane (MAO), purchased from Albemarle as a 10 wt % Al toluene solution, was first evaporated under vacuum at 50°C. It was then washed with distilled *n*-hexane twice and was finally dried in vacuum and stored as white powder in glovebox (dried MAO, dMAO).[22,23]

Scheme 1 shows the structure of the catalyst complex used in this work, bis[N-(3-methylsalicylidene)−2,3,4,5,6-pentafluoroanilinato] titanium(IV) dichloride. The synthesis was performed following to the literature.[24]

Ethylene/1-octene copolymerization

A 500-mL three-necked glass bottle with a Teflon mechanical stirrer was used to carry out polymerization. The ethylene consumption rate was recorded by a Brooks 5860E mass flow meter. Data acquisition was performed by a PCI8735 data acquisition card on the PC mother board, which could linearize the analog output of 4–20 mA from the mass flow meter.

The catalyst and cocatalyst dMAO toluene solutions were freshly prepared prior to each experiment. The reaction temperature was controlled at 25°C by a water bath. The reactor was thoroughly dried before anhydrous toluene was charged through a vacuum hose. The toluene was then stirred (600 rpm) under an ethylene atmosphere. A predetermined amount of 1-octene was injected into the reactor followed by the addition of dMAO solution. The polymerization was started by injecting the catalyst solution. Once the catalyst was injected, the ethylene consumption rate was recorded immediately. Ethylene was fed continuously to maintain the constant pressure of 1 atm during the reaction. To synthesize block copolymers, 1-octene was fed to the reactor in a stepwise fashion, following the designed feeding policy. After the preset reaction time, the polymerization was terminated by shutting off ethylene feeding and by injecting 10-mL alcohol. The resulting mixture was poured into acidified alcohol (2 vol % of hydrochloric acid). After filtration, washed with excess alcohol, the polymer sample was finally dried in vacuum at 50°C for 8 h.

Characterization

Molecular weight (M_w and M_n) and polydispersity index (PDI) of the copolymers were analyzed by high-temperature gel permeation chromatography (GPC). A PL-GPC 220 system equipped with an in-line capillary viscometer was used in this work. The column was calibrated with monodisperse polystyrene (PS) standards. The Mark–Houwink constants for universal calibration were $K = 5.91 \times 10^{-4}$ and $\alpha = 0.69$ for PS, and $K = 1.21 \times 10^{-4}$ and $\alpha = 0.707$ for PE. The solvent of 1, 2, 4-trichlorobenzene was pumped at a flow rate of 1.0 mL/min at 150°C.

Copolymer composition was determined by ^{13}C NMR spectra. Solutions with 10 wt % polymer in deuterated o-dichlorobenzene were prepared at 150°C. It was scanned at 125°C using a Bruker AC 400-pulsed NMR spectrometer. Instrument conditions, such as 90° pulse angle, inverse-gated proton decoupling, and 8000-Hz spectral width, were

Table 1. Kinetic Model for Living Ethylene/1-Octene Copolymerization

	Element Reactions
Initiation	$C^* + M_j \xrightarrow{k_{ij}} P^*_{1,j}$ $j = 1,2$
Propagation	$P^*_{n,1} + M_1 \xrightarrow{k_{p21}} P^*_{n+1,1}$
	$P^*_{n,2} + M_1 \xrightarrow{k_{p12}} P^*_{n+1,1}$
	$P^*_{n,1} + M_2 \xrightarrow{k_{p22}} P^*_{n+1,2}$
	$P^*_{n,2} + M_2 \xrightarrow{k_{p11}} P^*_{n+1,2}$
Chain transfer to Al	$P^*_{n,i} + Al \xrightarrow{k_{tAl}} C^* + D_n$
Deactivation	$P^*_{n,i} \xrightarrow{k_d} C_d + D_n$
Species	
C^*: active centers	$P^*_{n,i}$: living polymer chains with n repeat D_n
C_d: inactive catalyst	Units and with last inserted i monomer
M_1: ethylene	D_n Dead polymer chains with n repeat units
M_2: 1-octene	Al: alkyl-aluminum in the cocatalyst

optimized for quantitative NMR. The pulse delay time was 8 s and acquisition time was 1.3 s. Approximate 5000 scans were collected for a good signal to noise ratio. The carbon assignments and the composition calculation of the copolymers were performed using ASTM D5017-96 method.[25]

Thermal properties of the copolymers were measured by TA Q200 thermal analyzer under N_2 atmosphere. To remove thermal history, samples of 5.0–7.0 mg were first heated to 160°C at 30°C/min and remained isotherm at 160°C for 5 min. Recrystallization was then achieved by cooling the samples to −90°C at 10°C/min. The samples were reheated from −90 to 160°C at 10°C/min after isotherm at −90°C for 3 min. Crystallization temperature (T_c) was determined from the cooling curve. Glass transition temperature (T_g) and peak melting temperature (T_m) were determined from the second heating.

Model Development

The kinetic mechanism was summarized in Table 1, based on the following assumptions: (1) activation of complex and cocatalyst is instantaneous; (2) chain growth is initiated by insertion of the first ethylene unit ($k_{i2} = 0$); and (3) chain transfer reactions to 1-octene are absent in this living catalyst system. As the penultimate effect was found minor for this copolymerization system,[21] the terminal model was suitable for the monomer insertion mechanism.

The average chain lengths are calculated from the method of moment. The i-th order moments are defined as follows

$$P^i_1 = \sum_{n=1}^{\infty} n^i \left[P^*_{n,1}\right];\ P^i_2 = \sum_{n=1}^{\infty} n^i \left[P^*_{n,2}\right];\ D^i = \sum_{n=1}^{\infty} n^i [D_n] \quad (1)$$

Mass balance equations are as follows

Active catalyst sites

$$d[C^*]/dt = k_{tAl}\left(P^0_1 + P^0_2\right)[Al] - k_{i1}[C^*][M_1] - k_{i2}[C^*][M_2] \quad (2)$$

Deactivated catalyst sites

$$d[C_d]/dt = k_d\left(P^0_1 + P^0_2\right) \quad (3)$$

$$[C^*]_0 = [C_d] + [C^*] + P^0_1 + P^0_2 \quad (4)$$

Monomers

$$d[M_1]/dt = q_{in} - \left(k_{i1}[C^*] + k_{p11}P^0_1 + k_{p21}P^0_2\right)[M_1] \quad (5)$$

$$d[M_2]/dt = -\left(k_{i2}[C^*] + k_{p12}P^0_1 + k_{p22}P^0_2\right)[M_2] \quad (6)$$

Zero-order moments for the living and dead polymer chains

$$dP^0_1/dt = k_{i1}[C^*][M_1] + k_{p21}P^0_2[M_1] - k_{p12}P^0_1[M_2] - (k_{tAl}[Al] + k_d)P^0_1 \quad (7)$$

$$dP^0_2/dt = k_{i2}[C^*][M_2] + k_{p12}P^0_1[M_2] - k_{p21}P^0_2[M_1] - (k_{tAl}[Al] + k_d)P^0_2 \quad (8)$$

$$dD^0/dt = (k_{tAl}[Al] + k_d)\left(P^0_1 + P^0_2\right) \quad (9)$$

First-order moments for the living and dead polymer chains

$$dP^1_1/dt = k_{i1}[C^*][M_1] + k_{p11}P^0_1[M_1] + k_{p21}\left(P^1_2 + P^0_2\right)[M_1] - k_{p12}P^1_1[M_2] - (k_{tAl}[Al] + k_d)P^1_1 \quad (10)$$

$$dP^1_2/dt = k_{i2}[C^*][M_2] + k_{p22}P^0_2[M_2] + k_{p12}\left(P^1_1 + P^0_1\right)[M_2] - k_{p21}P^1_2[M_1] - (k_{tAl}[Al] + k_d)P^1_2 \quad (11)$$

$$dD^1/dt = (k_{tAl}[Al] + k_d)\left(P^1_1 + P^1_2\right) \quad (12)$$

Second-order moments for the living and dead polymer chains

$$dP^2_1/dt = k_{i1}[C^*][M_1] + k_{p11}\left(2P^1_1 + P^0_1\right)[M_1] + k_{p21}\left(P^2_2 + 2P^1_2 + P^0_2\right)[M_1] - k_{p12}P^2_1[M_2] - (k_{tAl}[Al] + k_d)P^2_1 \quad (13)$$

$$dP^2_2/dt = k_{i2}[C^*][M_2] + k_{p22}\left(2P^1_2 + P^0_2\right)[M_2] + k_{p12}\left(P^2_1 + 2P^1_1 + P^0_1\right)[M_2] - k_{p21}P^2_2[M_1] - (k_{tAl}[Al] + k_d)P^2_2 \quad (14)$$

$$dD^2/dt = (k_{tAl}[Al] + k_d)\left(P^2_1 + P^2_2\right) \quad (15)$$

The ethylene pressure and reaction temperature remain invariable during the reaction and the ethylene concentration is thus assumed to be constant. Ethylene reaction rate was the same as the ethylene consumption rate. 1-Octene conversion is calculated according to Eq. 18. The average 1-octene incorporation is calculated from Eq. 19. The molecular weights (M_n and M_w) are calculated from Eqs. 22 and 23

$$R_{p1} = q_{in} = \left(k_{i1}[C^*] + k_{p11}P^0_1 + k_{p21}P^0_2\right)[M_1] \quad (16)$$

$$R_{p2} = -d[M_2]/dt = \left(k_{i2}[C^*] + k_{p12}P^0_1 + k_{p22}P^0_2\right)[M_2] \quad (17)$$

$$X_2 = \int R_{p2}dt/[M_2]_0 \quad (18)$$

$$\bar{F}_2 = \int R_{p2}dt \Big/ \left(\int R_{p2}dt + \int R_{p1}dt\right) \quad (19)$$

$$\bar{P}_n = \left(P^1_1 + P^1_2 + D^1\right)/\left(P^0_1 + P^0_2 + D^0\right) \quad (20)$$

$$\bar{P}_w = \left(P^2_1 + P^2_2 + D^2\right)/\left(P^1_1 + P^1_2 + D^1\right) \quad (21)$$

$$M_n = \bar{P}_n[m_1(1 - \bar{F}_2) + m_2\bar{F}_2] \quad (22)$$

$$M_w = \bar{P}_w[m_1(1 - \bar{F}_2) + m_2\bar{F}_2] \quad (23)$$

$$\text{PDI} = M_w/M_n \quad (24)$$

Results and Discussion

Parameters estimation

The kinetic parameters were estimated from correlating the model to experiment data by a least-square method using Matlab 2008b. The initial conditions of the above ordinary differential equations were set to zero, except for the catalyst, cocatalyst, ethylene, and 1-octene concentrations. The monomer reactivity ratios were cited from our previous work.[21] The online ethylene consumption rate and the end-of-batch measured molecular weight under solution

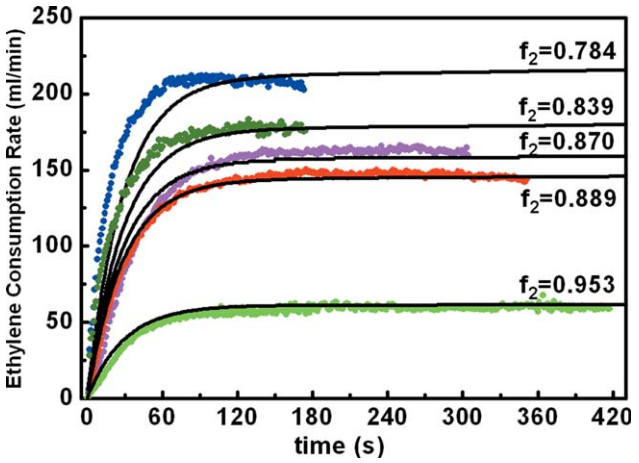

Figure 1. Online ethylene consumption rate (•) and model correlation for the parameter estimation.

[Color figure can be viewed in the online issue, which is available at wileyonlinelibrary.com.]

conditions (at $f_2 > 0.77$) were used to estimate the kinetic parameters through the model correlation of the experimental data in Ref. 21. Figure 1 shows the model fits to the ethylene reaction rates. The estimated parameters are listed in Table 2. The experimental and model calculated values of $\bar{F}_2$, M_w, and PDI are compared in Table 3. All the experimental data in Table 3 were cited from Ref. 21.

The assumption of $k_{i2} = 0$ indicated that the chain propagation was hardly initiated by 1-octene comonomer in this catalyst system. The smaller k_{i1} than k_{p11} in Table 2 supported the hypothesis that the insertion of the first ethylene unit was slow.[26] In other words, the insertion of the first ethylene unit was the rate limiting step in the chain growth. The much smaller k_{p21} than k_{p11} was attributed to steric hindrance of 1-octene unit to the incoming ethylene monomer.[21] This accounted for the ethylene consumption rate reduction at high 1-octene concentrations. The value of k_{p22} was around 46 L mol^{-1} S^{-1}, reflecting the poor ability of the FI-Ti catalyst in 1-octene homopolymerization. Our experiments also confirmed that the FI catalyst used in this work has almost no activity in 1-octene homopolymerization.

The estimated parameters were used to predict new results under different polymerization conditions. The experiment data of Runs 6, 7, and 8 were not used in the parameter estimation and were thus used for this model validation purpose.

Table 2. Kinetic Parameters Estimated from Ethylene Reaction Rate and Molecular Weights

Parameter	Unit	Value
k_{i1}	L mol^{-1} S^{-1}	13
k_{i2}	L mol^{-1} S^{-1}	0
k_{p11}	L mol^{-1} S^{-1}	3.70e4
k_{p21}	L mol^{-1} S^{-1}	1.36e3
r_1 (k_{p11}/k_{p12})		55
r_2 (k_{p22}/k_{p21})		0.034
k_{tAl}	L mol^{-1} S^{-1}	2.5
k_d	S^{-1}	1.0e-4

These runs were in a slurry condition. Table 3 shows that the model agreed well with most experimental data. In general, M_w decreased as f_2 increased (Runs 1, 2, and 6, reaction time = 3 min; Runs 3, 7, and 8, reaction time = 5 min). This was attributed to the decreased ethylene reaction rate at increased f_2. Figure 2 shows the ethylene consumption rate. Again, the model fits the data well. The kinetic parameters estimated from solution conditions were still useful in predicting the slurry polymerization results. This was because the mass-transfer effect was not dominating in the slurry polymerization. The solid content was controlled below 3 wt %. As reported in the literatures,[27,28] the mass-transfer effect could be minimized by applying high agitation speed and controlling polymer solid content below 15 wt %. Figure 3 shows that the model simulated 1-octene reaction rate increased with the 1-octene concentration, agreeing with the increase of 1-octene activity with f_2.[21] This simulation result provides information that 1-octene was consumed at a stable rate in this living copolymerization system. Figure 4 also shows the good agreement between model and experimental $\bar{F}_2$ and M_w results.

Ethylene/1-octene copolymer with uniform composition

In a batch process, variations in comonomer concentration over the course of polymerization often result in copolymer composition drifting. In a living copolymerization system, the composition drift is not from chain to chain, but from end to end of individual chains. However, in this work, 1-octene conversion was controlled at a low level (<5%). The change in the 1-octene concentration was small and negligible, giving a stable comonomer feeding ratio during the reaction. Although the instantaneous 1-octene polymerization rate (R_{p2}) could not be measured experimentally, the conversion of 1-octene could be measured by combining the NMR analysis, 1-octene feed, and weight of copolymer product. Figure 5 shows the model prediction for a linear increase of 1-octene conversion X_2 with reaction time, which was verified by the experimental

Table 3. Experimental Data and Model Calculation Results at Different f_2

		$\bar{F}_2$ (%)			M_w (e4g/mol)			PDI		
Run No[a]	f_2	Exp.	Model	δ[b](%)	Exp.	Model	δ(%)	Exp.	Model	δ (%)
1	0.784	6.3	6.5	3.2	27.34	29.34	7.3	1.11	1.17	5.4
2	0.839	10.1	9.3	−7.9	22.07	19.90	−9.8	1.13	1.08	−4.4
3	0.870	11.4	11.6	1.8	25.25	24.27	−3.9	1.10	1.09	−0.9
4	0.889	13.2	13.9	5.3	28.51	26.32	−7.7	1.15	1.10	−4.3
5	0.953	32.7	31.2	−4.6	25.30	27.80	9.9	1.16	1.07	−7.8
6	0.329	0.88	0.89	1.1	32.23	30.18	−6.4	1.20	1.17	−1.7
7	0.655	3.5	3.4	−2.9	35.09	36.60	4.3	1.15	1.18	2.6
8	0.736	4.9	5.0	2.0	31.65	32.01	1.1	1.14	1.15	0.9

[a]Experimental data cited from Ref. 21.
[b]Relative errors.

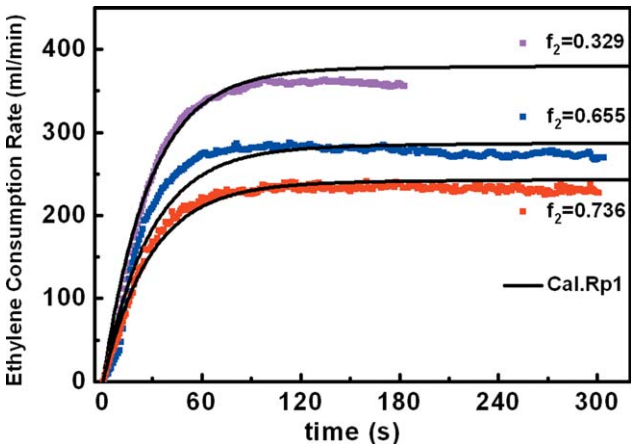

Figure 2. Experimental data (■) and model predictions of ethylene consumption rate at different f_2.

[Color figure can be viewed in the online issue, which is available at wileyonlinelibrary.com.]

data from Ref. 21. This linear increase was consistent with the approximately constant 1-octene reaction rate, as simulated in Figure 3. Figure 6 shows the variation of 1-octene incorporation $\bar{F}_2$ with the number average chain length. Although 1-octene was introduced into the system in a batchwise process, $\bar{F}_2$ was independent from the chain length. The copolymer composition drifting was avoided at low 1-octene conversions in the batch living copolymerization.

Figure 7 shows the copolymer molecular weight M_w increased continuously within the studied reaction time, whereas the PDI values remained to be low, characteristic of the living copolymerization behavior.

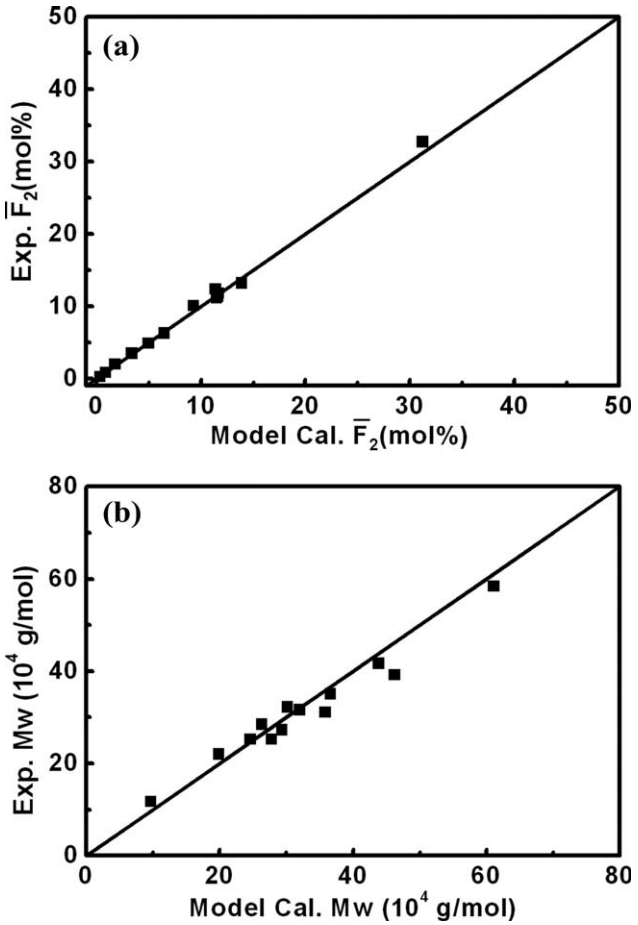

Figure 4. Comparison between model and experimental results, (a): $\bar{F}_2$ and (b): M_w.

Synthesis of ethylene/1-octene block copolymers

Living coordination polymerization is particularly useful in synthesizing olefin block copolymers. Ethylene/1-octene block copolymers were prepared in this work. The objective was to illustrate use of the model simulation in synthesis of tailor-made polyolefin chain microstructure. Scheme 2 shows the targeted block structures. In this work, we set the constraint conditions for a diblock copolymer

$$\text{Diblock}: \begin{cases} \bar{F}_2 = 0.9\%, & \bar{P}_n \le 6300 \\ \bar{F}_2 > 17\%, & \bar{P}_n > 6300 \end{cases} \tag{25}$$

and a triblock copolymer

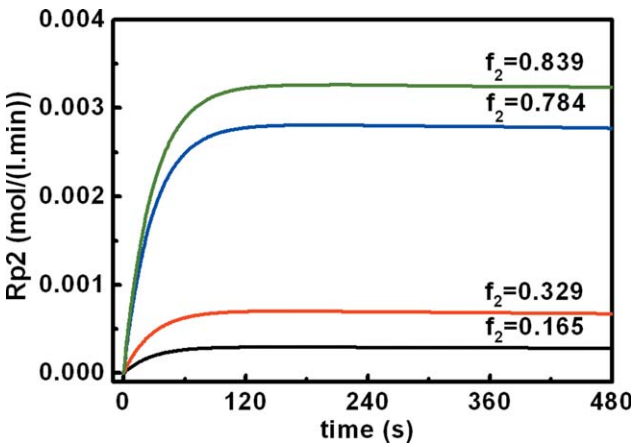

Figure 3. Model predicted 1-octene reaction rate at different f_2.

[Color figure can be viewed in the online issue, which is available at wileyonlinelibrary.com.]

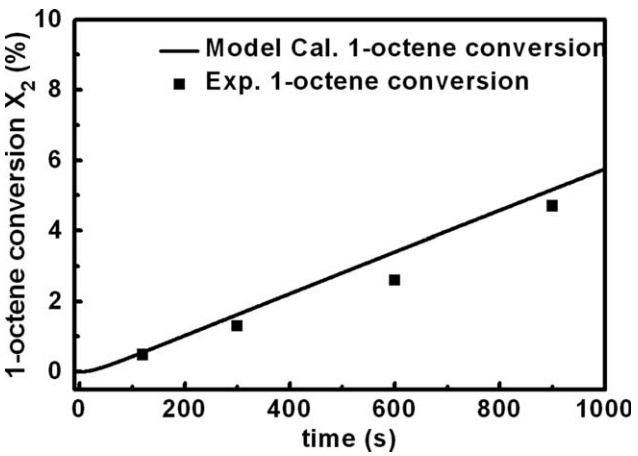

Figure 5. Evolution of 1-octene conversion with reaction time, $f_2 = 0.870$.

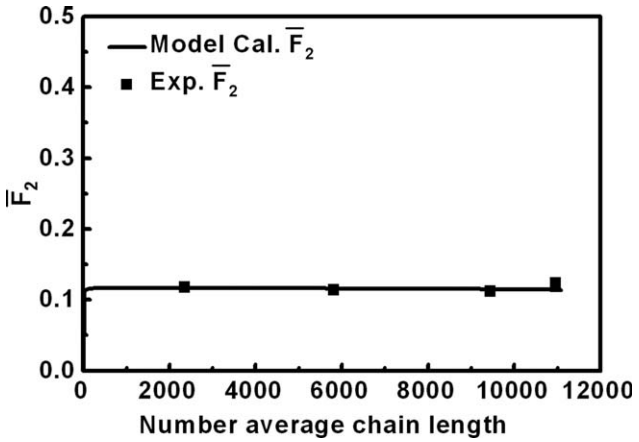

Figure 6. Evolution of $\bar{F}_2$ with number-average chain length, $f_2 = 0.870$.

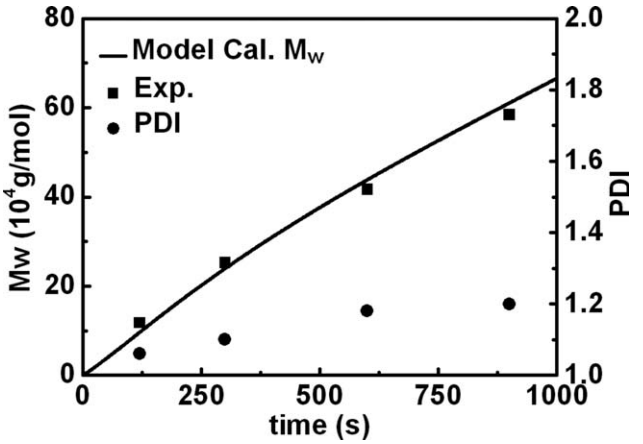

Figure 7. Evolution of M_w and PDI with reaction time, $f_2 = 0.870$.

$$\text{Steptriblock}: \begin{cases} \bar{F}_2 = 0.9\%, \ \bar{P}_n \le 6300 \\ \bar{F}_2 = 5.8\%, \ 6300 < \bar{P}_n \le 11500 \\ \bar{F}_2 > 17\%, \ \bar{P}_n > 11500 \end{cases} \quad (26)$$

as examples. It should be pointed that in theory any constraints could be proposed. But in practice, we need to consider operation conditions. The degree of polymerization 6300 corresponded to 2 min in operation at the composition, whereas it was 3 min from 6300–11,500. It is difficult to experiment for too long and too short time in operation.

In synthesis of this type of olefin block copolymers, a small fraction of 1-octene was precharged to the reactor. Mayo–Lewis equation was used to calculate the 1-octene loads for targeted copolymer composition ($\bar{F}_2$). For the diblock copolymers, 1-octene was fed in two stages. The 1-octene feeding ratio curve (f_2 vs. time) is shown in Figure 8a. The f_2 was initially maintained at 0.329 for 2 min and was subsequently increased to 0.889 and continued for additional 10 min, to obtain the desired molecular weight and diblock structure. Table 4 gives the recipes for the synthesis of ethylene/1-octene diblock copolymers. Run 9 was used as a control experiment.

Figure 8b shows the ethylene consumption rate. It decreased in a stage-wise manner as 1-octene was fed sequentially, showing significant influence of 1-octene on the rate of ethylene consumption. The model prediction matched well with experimental data. The model-data mismatch during the transition period was mainly introduced by experimental operation. In the actual operation, it took a few seconds to inject the large volume of 1-octene (nearly 50 mL). Once the 1-octene concentration reached stable, the model prediction matched well with experimental data. Figure 8c shows GPC curves of the copolymer samples from Runs 9 and 11. The molecular weight of Run 11 increased significantly from that of Run 9, confirming the chain extension at a higher 1-octene concentration in the second step. Figure 8d shows the NMR spectrum and Table 5 gives the triad sequence length distributions of the copolymers. Comparing Run 11 to Run 9, the fractions of [EEO+OEE], [OEO], [EOE], and [EOO+OOE] obviously increased and the fraction of [EEE] decreased, showing that the comonomer incorporation increased in the second step. The evolution of molecular weight and comonomer incorporation confirmed the diblock structure for the copolymer from Run 11. Figure 8e shows the evolution of molecular weight and polydispersity with polymerization time. The model correlated nicely with the experimental results. Figure 8f shows the variation of cumulative copolymer composition with the number-average chain length. $\bar{F}_2$ is the average composition of the total copolymer, whereas $\bar{F'}_2$ is the average composition in each block, which can be calculated from $\bar{F}_2$ and M_n. As 1-octene was fed stage-wisely, the increase of the block average was also in a stage-wise manner. The model captured this trend and agreed with the experimental results.

In the synthesis of step triblock copolymers, 1-octene was fed gradually in three stages, as shown in Figure 9a: f_2 was maintained at 0.329 for 2 min, then increased to 0.736 for 3 min, and finally to 0.889 for 7 min. The recipe was also summarized in Table 4. Run 12 was used as a control experiment. Figure 9b shows the ethylene consumption rate

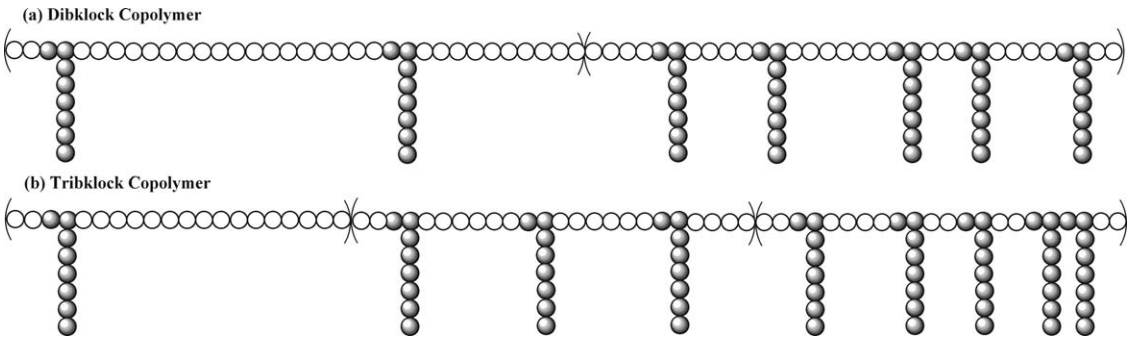

Scheme 2. Schematic illustration of chain structure of diblock (a) and (b) step triblock copolymers.

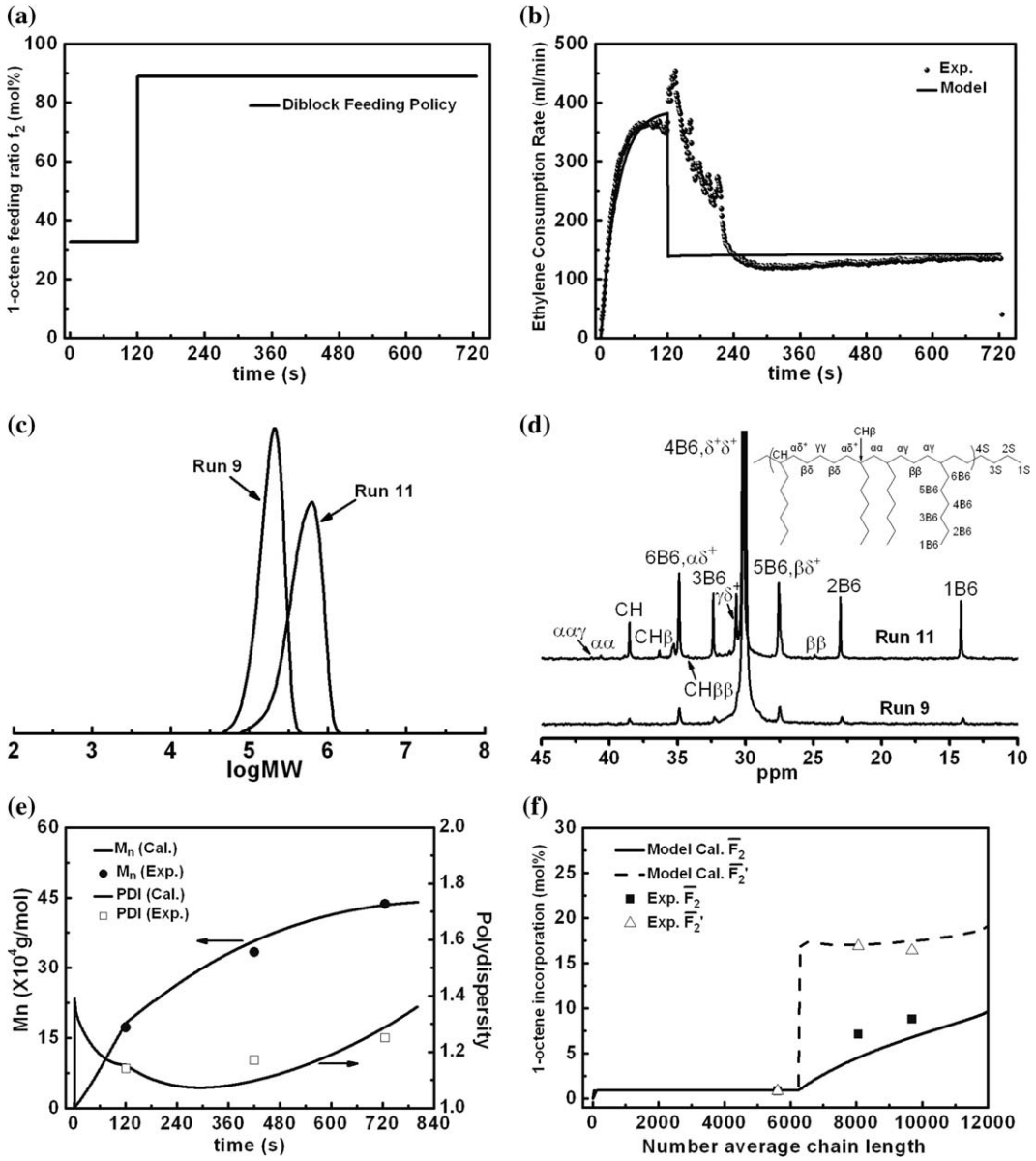

Figure 8. Synthesis of ethylene/1-octene diblock copolymer: (a) 1-octene feeding ratio with reaction time; (b) online ethylene consumption rate with experimental data (•) from Run 11 and model result (-); (c) GPC curve; (d) ^{13}C-NMR spectrum; (e) molecular weight and polydispersity vs. reaction time; (f) cumulative copolymer composition vs. number-average chain length, F_2 is the total 1-octene incorporation in the final block copolymer, $\bar{F}'_2$ is the 1-octene incorporation in each block, calculated from $\bar{F}_2$ and M_n.

vs. time. The model agreed well with the experimental result. Figure 9c shows the GPC curves from Runs 9, 12, and 14, confirming the chain extension after each step. The NMR spectrum in Figure 9d and the results of triad sequence length distributions in Table 5 also demonstrated that the comonomer incorporation increased after each step,

Table 4. Recipes for the Synthesis of Ethylene/1-Octene Block Copolymers

Run[a]	Targeted Copolymers	First Block f_2	First Block, t (min)	Second Block f_2	Second Block, t (min)	Third Block f_2	Third Block, t (min)
9	Random	0.329	2	–	–	–	–
10	Diblock	0.329	2	0.889	5	–	–
11	Diblock	0.329	2	0.889	10	–	–
12	Diblock	0.329	2	0.736	3	–	–
13	Triblock	0.329	2	0.736	3	0.889	3
14	Triblock	0.329	2	0.736	3	0.889	7

[a]Reaction condition: P = 1 atm, T = 25°C, complex [Ti] = 20 μmol/l, Al/Ti = 2000, toluene = 210 mL.

Table 5. The Triad Sequence Length Distributions for Ethylene/1-Octene Copolymers Determined by ^{13}C-NMR

Run No.	$\bar{F}_2$ (%)	EEE (%)	EEO + OEE (%)	OEO (%)	EOE (%)	EOO + OOE (%)	OOO (%)
9	0.83	94.4	4.14	0.566	0.852	0	0
10	7.1	83.6	7.70	0.750	5.23	2.69	0
11	8.8	78.9	13.0	0.771	5.69	1.69	0
12	3.2	93.2	3.73	0.058	2.65	0.392	0
13	5.3	88.0	6.18	0.783	3.60	1.44	0
14	8.3	81.1	10.8	1.66	4.81	1.61	0

confirming the triblock structure from Run 14. Figure 9e shows the molecular weight and polydispersity with time. It is evident that the model and experiment results agreed well with each other. Figure 9f shows the variation in cumulative composition of the triblock copolymer with number-average chain length. Each block segment had a different composition and presented a step variation as the model simulated. The composition distributions of the first and second blocks were uniform. However, the third block gave a gradient distribution profile. This was because the chains grew very slowly in the third block and thus inevitably involved chain transfer reactions, which led to formation of dead chains and

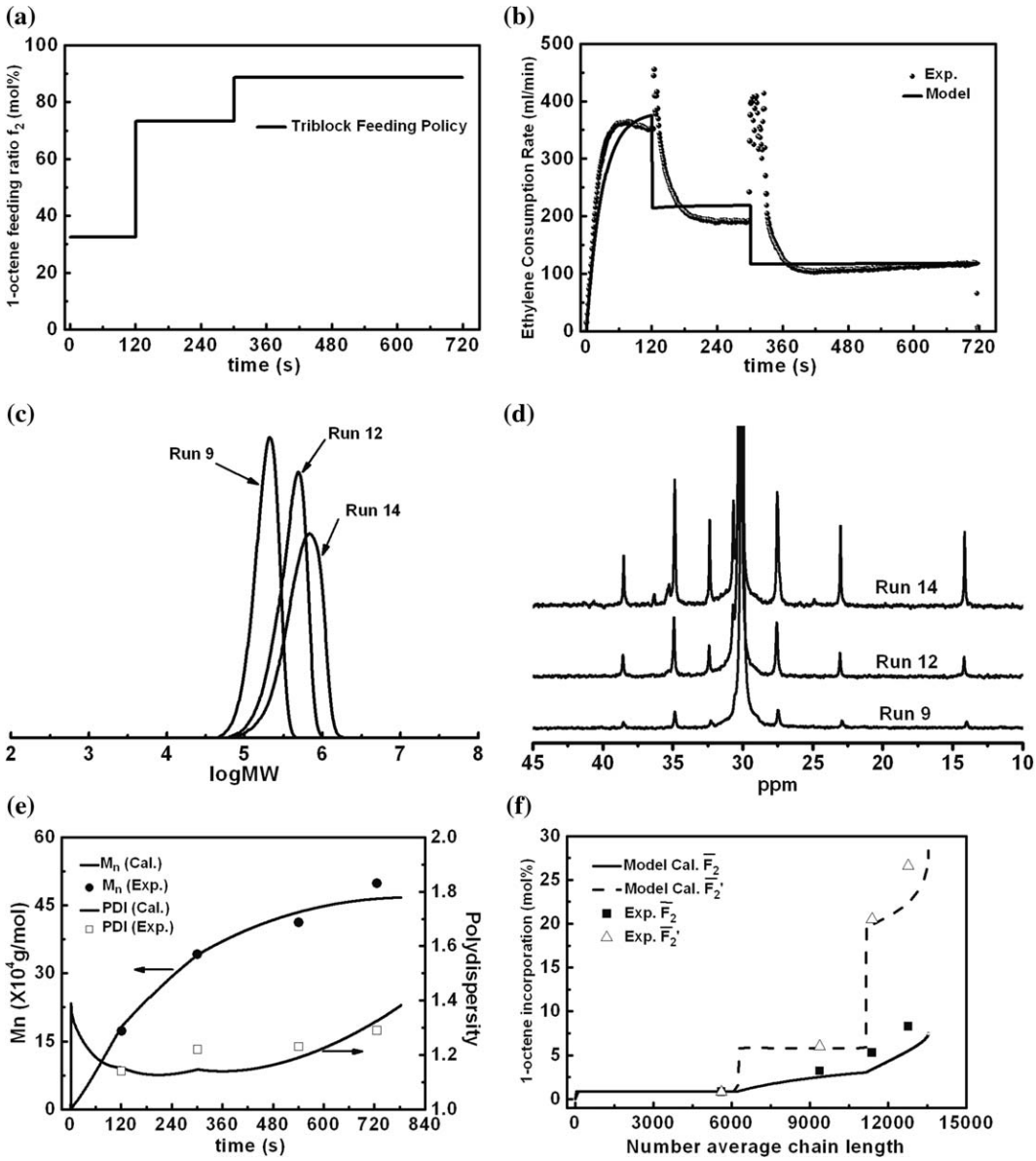

Figure 9. Synthesis of step triblock ethylene/1-octene copolymer: (a) 1-octene feeding ratio with reaction time; (b) online ethylene consumption rate with experimental data (•) and model result (-); (c) GPC curves; (d) ^{13}C-NMR spectrum; (e) molecular weight and polydispersity vs. reaction time; (f) cumulative copolymer composition vs. number-average chain length, $\bar{F}_2$ is the overall 1-octene incorporation in the final block copolymer, $\bar{F}_2^i$ is the 1-octene incorporation in each block, calculated from $\bar{F}_2$ and M_n.

generation of new chains. The model revealed these experimental features.

Figures 8 and 9 show that the block copolymers had the exact composition distributions and molecular weights as the model simulated, demonstrating good control over the polyolefin chain microstructure.

Thermal properties of the block copolymers

Some thermal properties of the synthesized block copolymers were studied by DSC analysis, with the random copolymer counterparts for comparison. The T_g, T_c, and T_m data are summarized in Table 6. The heat of melting ΔH_m was used to evaluate crystallinity, with $\Delta H_m^0 = 290$ J/g as reference for infinite polyethylene crystal.[29] Both high T_m and low T_g were retained in the block copolymers, as shown in Figure 10. It is of interest to note that a bimodal melting curve was observed from the diblock copolymer (Run 11), and a trimodal melting curve was observed from the triblock copolymer (Run 14). This multimodality in melting behavior could be attributed to phase separation in the block copolymers. Each block was long enough to form a distinct phase. The 1-octene content in the hard block was only about 0.9 mol%, allowing the hard block to form plastic phase. Polyethylene chains in a plastic phase normally form spherulites,[30] giving the material a high T_m (113–114°C for the block copolymers in this work). The soft block with the 1-octene content higher than 17 mol % composed an amorphous rubbery phase, in which polyethylene chains could only form fringed micelles or bundled crystals with T_m around 40°C and T_g lower than −50°C.[31] The middle block in the triblock copolymer had around 6 mol % 1-octene, which might form a mixed transition phase possessing lamellar crystals and bundled crystals, rendering the triblock copolymer a middle melting summit at about 77°C.

The block copolymers clearly retained the crystallization capacity of the hard block, and thus possessed the high melting temperature, together with the low-glass transition temperature of the soft block.

Conclusions

In summary, a simple but useful kinetic model was developed for living ethylene/1-octene copolymerization. The model parameters were estimated from online ethylene consumption rate and end-of-batch molecular weight measurements. The model prediction agreed well with the experimental results. The estimated k_{i1} was much smaller than k_{p11}, suggesting that the insertion of first ethylene unit was the rate limiting step in the polyolefin chain growth. The comonomer concentration had significant influence on the rate of ethylene consumption. The much smaller k_{p21} than k_{p11} implied the steric hindrance of 1-octene unit to the incoming ethylene monomers, which accounted for the decrease in ethylene consumption rate with increased 1-octene concentration. The small k_{p22} value indicated poor ability of this catalyst system in 1-octene homopolymerization. The kinetic model with the estimated kinetic parameters was then used to simulate the chain microstructural properties of ethylene/1-octene copolymers with controlled uniform, diblock, and step triblock composition distributions, which were synthesized using semibatch sequential comonomer feeding policies. The resulting copolymers had the exact composition distributions and molecular weights as the model simulated. The block copolymers exhibited high melting temperature of the hard block and low-glass transition temperature of the soft block.

This work demonstrated that the polyolefin chain microstructure could be precisely controlled through semibatch comonomer feeding policies in living coordination polymerization. It was demonstrated that such chain properties could be predicted through modeling. Such design and control over chain microstructure allow us to tailor-make polyolefin materials.

Table 6. Summary of T_g, T_c, and T_m for Some Copolymers Determined by DSC

Run	T_g (°C)	T_c (°C)	T_m (°C)	ΔH_m (J/g)	X_c[a] (%)
4	−55.6	22.4	41.3	28	10
9	−32.4	103.6	117.7	112	39
11	−53.7	19.6, 99.2	39.9, 113.9	73	25
14	−53.1	19.8, 61.6, 99.3	39.3, 76.7, 113.0	87	30

[a]Crystallinity from heat of melting, taking ΔH_m^0 of 293 J/g for the polyethylene crystal.

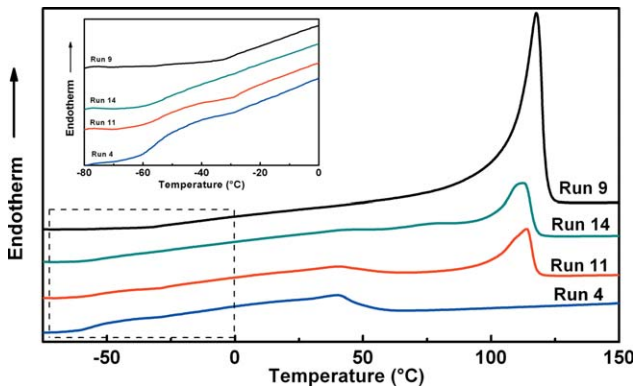

Figure 10. DSC melting curves of the block copolymers in comparison with the random copolymer counterparts.

The second heating was taken with the heating/cooling rate of 10°C/min. [Color figure can be viewed in the online issue, which is available at wileyonlinelibrary.com.]

Acknowledgments

The authors give grateful thanks to the supports from the National Natural Science Foundation of China (Nos. 20936006 and 20976152) and the National Basic Research Program of China (2011CB606001). The authors would also thank to Li Li, Kailun Zhang, and Zhiyang Bu at Zhejiang University for their kind assistance in this work.

Literature Cited

1. Takeuchi D. Recent progress in olefin polymerization catalyzed by transition metal complexes: new catalysts and new reactions. *Dalton Trans*. 2010;39:311–328.
2. Zhu S, Hamielec A. Polymerization kinetic modeling and macromolecular reaction engineering. In: Matyjaszewski K, Möller M, editors. Polymer Science: A Comprehensive Reference. Amsterdam: Elsevier BV, 2012:779–831.
3. Soares JBP. Mathematical modelling of the microstructure of polyolefins made by coordination polymerization: a review. *Chem Eng Sci*. 2001;56:4131–4153.
4. Mehdiabadi S, Soares JBP. Ethylene homopolymerization kinetics with a constrained geometry catalyst in a solution reactor. *Macromolecules*. 2012;45:1777–1791.

5. Kou B, McAuley KB, Hsu JCC, Bacon DW. Mathematical model and parameter estimation for gas-phase ethylene/hexene copolymerization with metallocene catalyst. *Macromol Mater Eng*. 2005;290: 537–557.
6. Zhang J, Fan H, Li BG, Zhu S. Modeling and kinetics of tandem polymerization of ethylene catalyzed by bis(2-dodecylsulfanyl-ethyl)amine-CrCl3 and Et(Ind)2ZrCl2. *Chem Eng Sci*. 2008;63: 2057–2065.
7. Dekmezian AH, Soares JBP, Jiang P, Garcia-Franco CA, Weng W, Fruitwala H, Sun T, Sarzotti DM. Characterization and modeling of metallocene-based branch-block copolymers. *Macromolecules*. 2002; 35:9586–9594.
8. Braunecker WA, Matyjaszewski K. Controlled/living radical polymerization: features, developments, and perspectives. *Prog Polym Sci*. 2007;32:93–146.
9. Sun X, Luo Y, Wang R, Li BG, Zhu S. Semibatch RAFT polymerization for producing ST/BA copolymers with controlled gradient composition profiles. *AICHE J*. 2008;54:1073–1087.
10. Luo Y, Wang X, Zhu Y, Li BG, Zhu S. Polystyrene-block-poly(n-butyl acrylate)-block-polystyrene triblock copolymer thermoplastic elastomer synthesized via RAFT emulsion polymerization. *Macromolecules*. 2010;43:7472–7481.
11. Wang R, Luo YW, Li BG, Zhu S. Control of gradient copolymer composition in ATRP using semibatch feeding policy. *AICHE J*. 2007;53:174–186.
12. Zhao Y, Luo YW, Ye C, Li BG, Zhu S. Model-based design and synthesis of gradient MMA/tBMA copolymers by computer-programmed semibatch atom transfer radical copolymerization. *J Polym Sci A Polym Chem*. 2009;47:69–79.
13. Domski GJ, Rose JM, Coates GW, Bolig AD, Brookhart M. Living alkene polymerization: new methods for the precision synthesis of polyolefins. *Prog Polym Sci*. 2007;32:30–92.
14. Zhang K, Ye Z, Subramanian R. Synthesis of block copolymers of ethylene with styrene and n-butyl acrylate via a tandem strategy combining ethylene "living" polymerization catalyzed by a functionalized Pd-diimine catalyst with atom transfer radical polymerization. *Macromolecules*. 2008;41:640–649.
15. Wang J, Zhang K, Ye Z. One-pot synthesis of hyperbranched polyethylenes tethered with polymerizable methacryloyl groups via selective ethylene copolymerization with heterobifunctional comonomers by chain walking Pd-diimine catalysis. *Macromolecules*. 2008;41: 2290–2293.
16. Mitani M, Mohri J, Yoshida Y, Saito J, Ishii S, Tsuru K, Matsui S, Furuyama R, Nakano T, Tanaka H, Kojoh S, Matsugi T, Kashiwa N, Fujita T. Living polymerization of ethylene catalyzed by titanium complexes having fluorine-containing phenoxy-imine chelate ligands. *J Am Chem Soc*. 2002;124:3327–3336.
17. Edson JB, Wang Z, Kramer EJ, Coates GW. Fluorinated bis(phenoxyketimine)titanium complexes for the living, isoselective polymerization of propylene: multiblock isotactic polypropylene copolymers via sequential monomer addition. *J Am Chem Soc*. 2008;130:4968–4977.
18. Makio H, Terao H, Iwashita A, Fujita T. FI catalysts for olefin polymerizations-a comprehensive treatment. *Chem Rev*. 2011;111: 2363–2449.
19. Furuyama R, Mitani M, Mohri J, Mori R, Tanaka H, Fujita T. Ethylene/higher α-olefin copolymerization behavior of fluorinated bis(phenoxy−imine)titanium complexes with methylalumoxane: synthesis of new polyethylene-based block opolymers. *Macromolecules*. 2005; 38:1546–1552.
20. Hotta A, Cochran E, Ruokolainen J, Khanna V, Fredrickson GH, Kramer EJ, Shin YW, Shimizu F, Cherian AE, Hustad PD, Rose JM, Coates GW. Semicrystalline thermoplastic elastomeric polyolefins: advances through catalyst development and macromolecular design. *Proc Natl Acad Sci USA*. 2006;103:15327–15332.
21. Liu W, Zhang K, Fan H, Wang WJ, Li BG, Zhu S. Living copolymerization of ethylene/1-octene with fluorinated FI-Ti catalyst. *J Polym Sci A Polym Chem*. 2013;51:405–414.
22. Cai Z, Ikeda T, Akita M, Shiono T. Substituent effects of tert-butyl groups on fluorenyl ligand in syndiospecific living polymerization of propylene with ansa-fluorenylamido dimethyltitanium complex. *Macromolecules*. 2005;38:8135–8139.
23. Itagaki K, Kakinuki K, Katao S, Khamnaen T, Fujiki M, Nomura K, Hasumi S. Tris(pyrazolyl)borate Ti(IV) complexes containing phenoxy ligands: effective catalyst precursors for ethylene polymerization that proceeds via cationic Ti(IV) species. *Organometallics*. 2009;28:1942–1949.
24. Mitani M, Furuyama R, Mohri JI, Saito J, Ishii S, Terao H, Nakano T, Tanaka H, Fujita T. Syndiospecific living propylene polymerization catalyzed by titanium complexes having fluorine-containing phenoxy-imine chelate ligands. *J Am Chem Soc*. 2003;125:4293–4305.
25. ASTM. ASTM D5017-96(2009) e1 Determination of Linear Low Density Polyethylene (LLDPE) Composition by Carbon-13 Nuclear Magnetic Resonance. West Conshohocken, PA: ASTM, 2009.
26. Thorshaug K, Støvneng JA, Rytter E, Ystenes M. Termination, isomerization, and propagation reactions during ethene polymerization catalyzed by Cp2Zr-R+ and Cp*2Zr-R+. An experimental and theoretical investigation. *Macromolecules*. 1998;31:7149–7165.
27. Gonzalez-Ruiz RA, Quevedo-Sanchez B, Laurence RL, Henson MA, Coughlin EB. Kinetic modeling of slurry propylene polymerization using rac-Et(Ind)2ZrCl2/MAO. *AICHE J*. 2006;52:1824–1835.
28. Quicker G, Schumpe A, Deckwer WD. Gas-liquid interfacial areas in a bubble column with suspended-solids. *Chem Eng Sci*. 1984;39: 179–183.
29. Wunderlich B. Macromolecular Physics. New York: Academic Press, 1980.
30. Minick J, Moet A, Hiltner A, Baer E, Chum SP. Crystallization of very low density copolymers of ethylene with a-olefins. *J Appl Polym Sci*. 1995;58:1371–1384.
31. Bensason S, Minick J, Moet A, Chum S, Hiltner A, Baer E. Classification of homogeneous ethylene-octene copolymers based on comonomer content. *J Polym Sci B Polym Phys*. 1996;34:1301–1315.

Manuscript received Apr 23, 2013, and revision received July 2, 2013.